Nanoscale

# Organic compound-based nanozyme for agricultural herbicide detection



| | |
|---|---|
| Journal: | *Nanoscale* |
| Manuscript ID | NR-ART-05-2023-002025.R2 |
| Article Type: | Paper |
| Date Submitted by the Author: | 11-Jul-2023 |
| Complete List of Authors: | Lee, Dong Hoon ; University of Illinois at Urbana-Champaign<br>Kamruzzaman, Mohammed; University of Illinois at Urbana-Champaign |
| | |

ARTICLE

# Organic compound-based nanozyme for agricultural herbicide detection

Received 00th May 2023
Accepted 00th January 20xx

DOI: 10.1039/x0xx00000x

Dong Hoon Lee,[a] and Mohammed Kamruzzaman [a*]

Nanozymes are increasingly being used in agricultural applications, but their adoption has been limited as these nanozymes are generally considered toxic, low cost-effectiveness, and complexity of fabrication. In this study, an organic compound-based, peroxidase-like nanozyme (OC nanozyme) was developed for use in the agricultural environment. This nanozyme was synthesized through a self-assembled one-pot particle synthesis process, interacting with the urea and the metalic ion to form the homogenous nanoparticle containing the partially mimicked cofactors (Fe-N) of the natural enzyme. The OC nanozyme exhibited decent kinetic properties ($H_2O_2$ / $K_m$:0.056mM and $V_{max}$:2.19 $\mu Ms^{-1}$) and decent pH stability. The OC nanozyme was successfully used to detect glyphosate via integrated colorimetric assay, with a decent limit of detection (LOD) of at least 0.001ngmL$^{-1}$. The authors envision that this agricultural–friendly OC nanozyme holds a great potential for a wide range of agricultural applications.

## Introduction

Nanozyme[1-5] has become a popular research subject in various disciplines, including biomedical, chemical engineering even agricultural engineering nowadays. One of the popular applications of nanozyme is biosensors, and researchers enable to integrate this nanozyme into the colorimetric or electrochemical readout platform to detect target molecules.[1,4] The catalytic activity of nanozyme facilitates the customization of cascade reaction chains for on-demand detection of various target molecules encompassing biological molecules or related small molecules. In recent years, researchers have also explored the use of nanozyme in agriculture and food science[6,7] to detect certain molecules based on their conventional nanozyme-substrate dependent reactions platform. These are effective, however, the materials that the researcher contrived are not ideal materials that may not be directly utilized in the agricultural and environmental aspects. Since a majority of nanozyme researchers utilized for agricultural applications are the conventional nanozyme; metal-based nanoparticles, engineered carbon structure, MOF (Metal-organic framework), and single atom nanozyme (SAN)[1,5,8], however, they are generally toxic and expensive materials to be utilized for agriculture. To strengthen the bio, eco-friendly aspect, researchers tried to manipulate the surface of the nanozyme to elevate its biocompatibility, but this is a transitory process and has yet to solve the problem entirely. Also, there are some examples of using MOF or SAN for agricultural biomolecule detection, but it is hard to apply the further real-world application as MOF or conventional SAN[2,8] nanozyme requires heavy fabrication steps and has low-cost effectiveness. To overcome this drawback, the novel nanozyme which is stable and eco-friendly, and has cost-effectiveness for agricultural applications, is desired. As most of the nanozyme deals with the dominant inorganic materials, it has been conceptualized to develop the organic nanoscale structure which follows the catalytic activity of the natural enzyme but structurally based on the organic compounds. Urea is one of the selected organic compounds with amino groups and carboxyl groups, they also can perform as the chelating agent of the metallic ion. Urea interacts with the iron ion and can promote the Fe-N bond, which partially mimics the cofactor of the natural peroxidase, to have a peroxidase-like activity. The particle stabilizer polyvinyl alcohol (PVA) participates in the particle generation process to form stable, spherical nanoparticles which become a novel organic compound-based nanozyme. Besides, there is a massive demand to detect pesticides or herbicides 'on demand', the researcher contrived nanozyme-based sensors to detect the pesticide/herbicide via colorimetric assay. The agricultural biomolecules detection using nanozyme are essential which lessens the process compared to the conventional analytical methods that give the potential for user-focused on-demand molecule monitoring applications. Among many agricultural biomolecules, glyphosate is selected as the target molecule for detection using OC nanozyme based colorimetric sensors.

Glyphosate is a widely used herbicide in the agricultural industry and detecting its presence in agricultural products can help prevent human damage and protect crop health[6,7,9,10,11].

[a] *Department of Agricultural and Biological Engineering, University of Illinois at Urbana-Champaign, Urbana, IL, 61801, USA, Email:mkamruz1@illinois.edu*

Electronic Supplementary Information (ESI) available: [details of any supplementary information available should be included here]. See DOI: 10.1039/x0xx00000x

In this study, the first example of the organic compound-based peroxidase-mimicking nanozyme (OC nanozyme) has been developed. The OC nanozyme has peroxidase-like activity and it has a decent kinetic profile with a considerably high eco-friendly aspect as all constituent materials are organic. The OC nanozyme has decent stability and cost-effectiveness compared to the natural enzymes and conventional types of nanozymes. It has been utilized in agricultural applications to detect glyphosate using a colorimetric assay. The OC nanozyme successfully detects the glyphosate with a decent LOD, providing its potential for further agricultural applications.

## Materials and methods

### Materials

Polyvinyl alcohol (MW 9K-10K) from Sigma-Aldrich (341584), Urea from Sigma-Aldrich (U5378), Iron(II) sulfate heptahydrate from Sigma-Aldrich (F8633), Sodium Acetate from Sigma Aldrich (236500), Acetic acid solution from Sigma-Aldrich (45474), ABTS (2,2'-Azino-bis(3-ethylbenzothiazoline-6-sulfonic acid) diammonium salt) from Sigma-Aldrich (A1888), Hydrogen Peroxide from Sigma-Aldrich, Glyphosate from Sigma-Aldrich (45521) were used as chemicals in the experiment.

### Morphological and chemical analysis

The analysis with operation were conducted at various facilities at the University of Illinois at Urbana-Champaign (UIUC), including Materials Research Lab (MRL), Beckman Institute, and the High throughput screening facility. STEM (Scanning Transmission Electron Microscope) images were characterized by a Tecnai G2 F20 S-Twin from Thermo Fisher Scientific, operating at a maximum 200 kV. SEM (Scanning Electron Microscopy) images were measured with a Hitachi S-4800 SEM, operating with an accelerating voltage of maximum 100 kV. XPS (X-ray photoelectron spectroscopy) measurements were conducted on a Kratos Axis ULTRA, with Al Kα x-ray radiation as the x-ray source for excitation. UV-VIS-NIR spectra data were obtained by Varian Cary 5G and Agilent Cary 5000. NTA (Nanoparticle tracking analysis) data was obtained from Nanosight NS300 from Malvern Panalytic, with sCMOS camera with blue488 laser. DLS/Zeta potential data were obtained from Malvern Zetasizer, Malvern Panalytic. FT-IR analysis profile were obtained from Nicolet is50 FTIR spectrometer, Thermo Fisher Scientific.

### Fabrication of organic compound-based nanozyme

The preparation of nanozyme involved several steps. Iron sulfate powder was dissolved in deionized water to achieve a final concentration of 1 $mgmL^{-1}$ at pH 4.8. PVA was dissolved in deionized water to a final concentration of up to 1 $mgmL^{-1}$. Urea was prepared as a 1 $mgmL^{-1}$ solution. A glass vial (10mL) was placed on a stirring plate and add 2 mL of the PVA solution was added to the vial. Then, 3 mL of Iron sulfate solution was added dropwise to the vial under stirring condition (180-200 rpm) for 10 minutes. Lastly, 4 mL of urea solution was added to the vial dropwise within fast stirring condition (280-300 rpm) and incubated the sample on the stirring condition up to 30 minutes. This vial was placed in a 4 °C refrigerator for up to 2 hours. The solution was then transferred to a 1.5 mL plastic tube and centrifuged at 25°C for 5 minutes at 5000 rpm. The supernatant was removed and washed using deionized water several times. Finally, the nanozyme at the bottom was resuspended with deionized water or buffer for further assay.

### Optimization and characterization of experimental condition

The experimental conditions were determined based on optimization and the previous reference (SI Ref 3). The different pH buffers/temperature buffers were prepared for the colorimetric assay to compare each performance directly (buffer=0.1M, sodium acetate). The performance was evaluated using absorbance spectroscopy, with the highest absorbance at 417 nm representing 100% endpoint, while the control buffer showed 0% endpoint. The entire experiment was conducted at a temperature of 25°C and a pH of 4, as these conditions provided the maximum absorbance endpoint.

### Peroxidase-like activity and its kinetic studies

Peroxidase activities were determined by ABTS-based colorimetric assays. Fifteen microliters of OC nanozyme (2.01e+14 M) and 15 µl hydrogen peroxide (final 100µM) and final 6mM ABTS were added into a 96 well plate containing 105 µl of sodium acetate–acetic acid buffer [70 mM final (pH 4.0)]. The other groups which displaced the hydrogen peroxide to deionized water and displaced from nanozyme to buffer were prepared parallelly. The catalytic oxidation of ABTS was studied by measuring the absorption changes of the oxidized form of ABTS at $\lambda_{max}$ = 417 nm. Absorbance spectra scanning was performed between λ =400 nm to 500 nm, repeating the measurements at least three times for each group. The steady-state kinetic profiles were determined by measuring the absorbance signal through the kinetic mode using Varian Cary 5G and Agilent Cary 5000. The 700 µl of NaAc buffer, and the 100 µl of OC nanozyme, 100 µl of Substrate (e.g. $H_2O_2$) and 100 µl of ABTS (varies from the concentration) were located on the cuvette to measure the consistent absorbance signal after 1 minute. Kinetic parameters were calculated by the Michaelis-Menten equation. Michaelis constant ($K_m$) and maximum initial velocity ($V_{max}$) were decreased from the Lineweaver-Burk plots and Michaelis-Menten equations, described as follows: $v = V_{max} \times [S] / (K_m + [S])$, where v is the initial velocity and [S] is the concentration of the substrate. The catalytic constant, known as $k_{cat}$, was calculated using the equation $k_{cat} = V_{max} / [E]$, where [E] is the molar concentration of Fe present in the OC nanozyme and it was calculated by the profile obtained from NTA analysis.

### Colorimetric detection of hydrogen peroxide

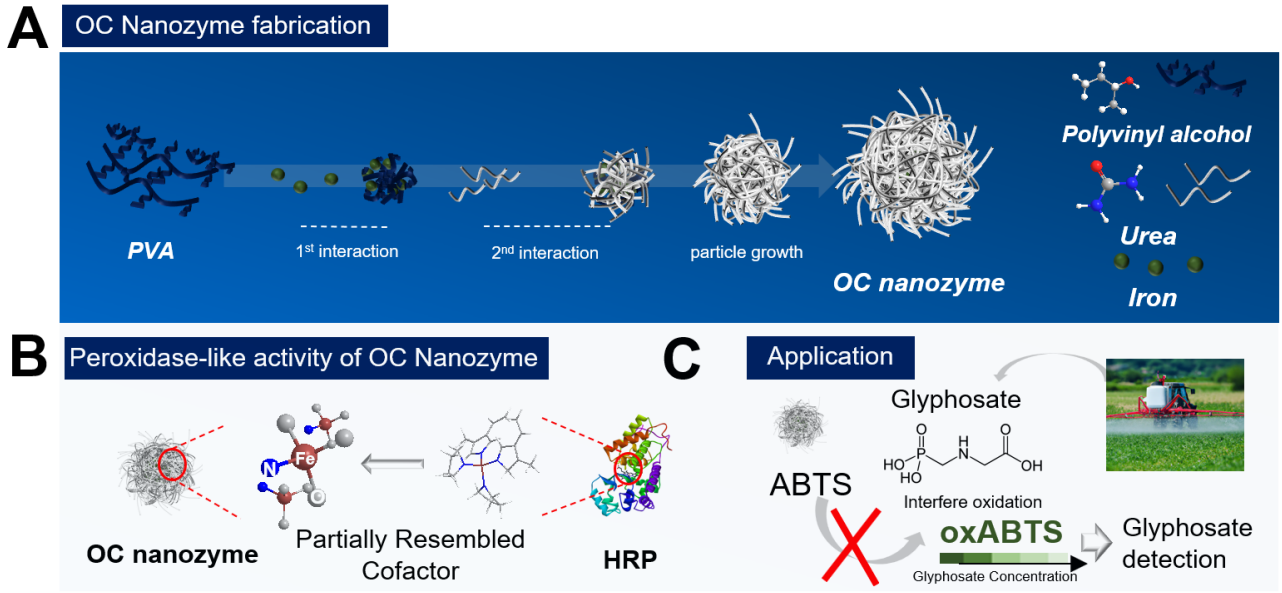


**Scheme 1** Schematic illustration of the OC nanozyme. A) Fabrication of the OC nanozyme, B) Partially mimicked heme cofactor (e.g., Fe-N) contained OC nanozyme, C) OC nanozyme for the agricultural herbicide detection.

Fifteen microliters OC nanozyme (around 2.01e+14 M) were added into a 96 well plate containing 105 µl of sodium acetate–acetic acid buffer [100 mM (pH 4.0)]. Then, 15 µl of varying concentrations of $H_2O_2$(10 nM to 1000µM) and 60 mM ABTS were added into the solution (oxABTS $\lambda_{max}$ = 417 nm). The catalytic oxidation of substrates was studied by measuring the absorption changes of the colorimetric assays undertake with TMB proceeded parallelly (if TMB = oxTMB ($\lambda_{max}$ = 652 nm)). The target timepoint was set at 5 minutes after all the chemicals were added to the 96 microwell plate.

### Sample preparation of Stability test

The OC nanozyme (around 2.01e+14 M) was dissolved in various pH buffer(2<pH<8.5) prepared by 0.1M sodium acetate. After incubation for 5 hours, the nanozyme was collected using a centrifuge (5000 rpm) and resuspend in pH 4 buffer (NaAc, 0.1M). The ABTS-based colorimetric assay was performed following the previously established procedure (endpoint) and calculated the relative stability based on the absorbance peak number.

### Glyphosate detection via colorimetric assay

Glyphosate was dissolved in deionized water and subjected to serial dilution to prepare various concentration of glyphosate. The column for the colorimetric assay for colorimetric assay was prepared according to previously established procedure using 0.1M pH 4 sodium acetate buffers and 1mM hydrogen peroxide. A 20 µl solution of glyphosate was added to the column and mixed the solution with the pipette. For the measurement, 6mM/final ABTS solution was added to the column. The measurement of glyphosate concentrations was performed using 96 well plate-based UV-VIS-NIR spectroscopy (Biotek 5 microplate reader). The endpoint analysis was conducted within 1 minute after adding all the chemicals to the 96 well plate. The absorbance spectra scanning was performed after 5 minutes. For the LOD measurement, 10 times lower concentration of the peroxidase was used to inhibit its fast oxidation of the ABTS and measured its absorbance on the scanning mode at 5 minutes after adding all the chemicals in the 96 well plate.

## Results and Discussion

### Morphological analysis of OC nanozyme

As illustrated in Scheme 1, the OC nanozyme was made by two major steps, the interaction between the functional group of the polymer and the iron ion. The second interaction with the urea was essential. The amino group from the urea formed a coordinate covalent bond with the iron and resulting in the consistent growth of its framework, and the final particle formed a spherical nanostructure with a solid unit (Figure S1). The particle growth happened due to the chelation of the iron; thus, this one-pot synthesis method did not require conventional nanoparticle fabrication methods, including heat increment. The morphological aspect was validated through STEM, SEM, and EDS (Energy-dispersive X-ray spectroscopy) analysis (Figure 1). The TEM and SEM image indicated that the OC nanozyme was spherical nanoparticle-like structure and the approximate diameter of the particle was around 200 nm (Figure 1 B, C, D). The presence of PVA, iron, and urea within the OC nanozyme was intentionally designed and the homogenious distribution of these components on the nanozyme was confirmed through EDS analysis. Urea was the only source for a nitrogen group and it was found that there were enriched nitrogen and iron signals from the EDS image (Figure 1 E). EDS image was visualized to exhibit a homogenous iron signal (Figure 1E) and the atomic ratio of iron, as quantified by EDS analysis, was determined to be 9.4% (Figure S2). Carbon and nitrogen were obtained from PVA and urea,

respectively. The atomic ratio of carbon was determined to be 35.7 % , while the atomic ratio of nitrogenwas found to be 11.9%. This indicated the homogeneity of the PVA and urea in the OC nanozyme indirectly (Figure S2). To understand the size and surface information of the OC nanozyme, DLS (Dynamic light scattering) and the zeta potential measurement were conducted. DLS profiles indicated that the OC nanozyme possessed a consistent size distribution with a mean size around 160 nm with decent polydispersity index (around 0.17) which implied its considerable homogeneity even though it is an organic compound-based nanoparticle (Figure S3A).

As the designated interaction of the urea was in the last steps, there is a higher possibility that the urea may be located on the surface of the whole structure; the zeta potential value was 4.85 mV (Figure S3B), which was positively charged due to the amino group from the urea. Prior to further analysis, another characterization was conducted related to the absorbance scanning with the OC nanozyme with two other organic compounds, PVA and urea to ascertain whether they exhibit intrinsic absorption at specific wavelengths. From this profile, there was no significant absorption on the Vis-NIR range, for all elements (Figure S4). The nanoparticle tracking analysis was conducted to examine the particle information of the OC nanozyme, particularly, the concentration of the nanozyme, for further assays. The estimated concentration of nanozyme was obtained and calculated to a molar concentration around 2.01e+14 M.

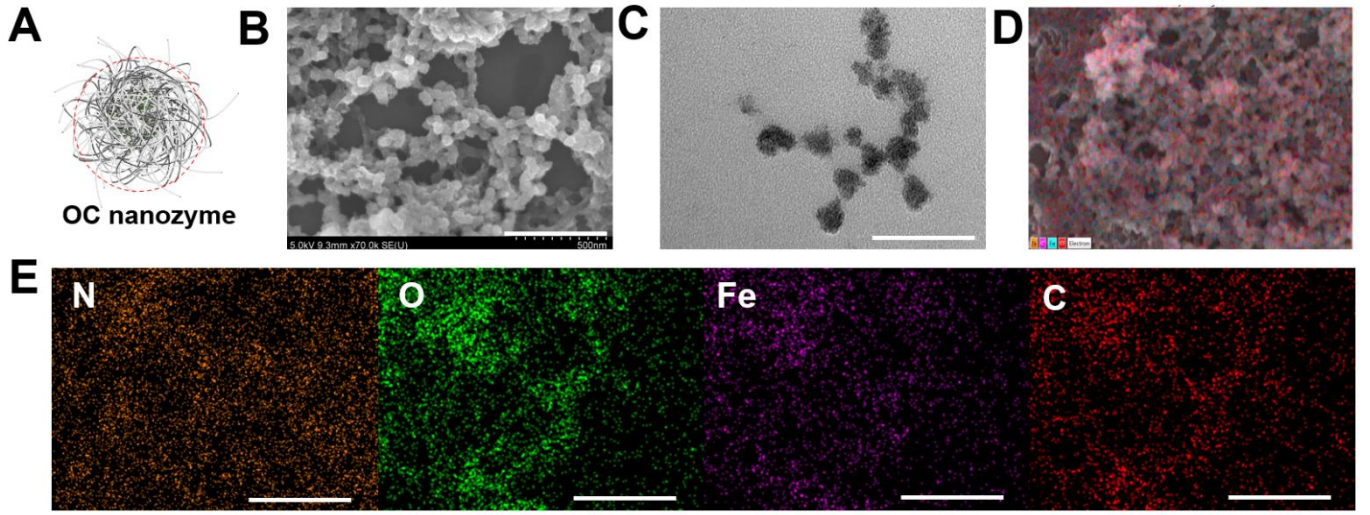


**Fig. 1** Morphological analysis of OC nanozyme. A) illustrates schematic of the OC nanozyme and its spherical structure, B) SEM image (scale bar: 500nm), C) Bright field TEM image (Scale: 150nm), D) EDS scanning spot from SEM image,. E) EDS mapping image with the elements, Carbon, Oxygen, Nitrogen, and Iron (Scale bar: 1µm)

As it has been argued that the OC nanozyme contains a partially mimicked cofactor of the natural enzyme, further characterization was conducted to find the inner bond within the OC nanozyme. The heme-cofactor model structure was selected as the OC nanozyme aims to resemble the natural peroxidase's cofactor, which have iron ions with its supporting ligands including nitrogen. XPS analysis was chosen to understand the chemical bonds of each element. The XPS survey revelaled the presence of several elements enriched in the OC nanozyme. The four elements with orbitals, C1s, N1s, O1s, and Fe2p were selected (Figure 2) and their XPS quantification-derived atomic ratio were 60.03, 4.52, 34.63, and 0.83, respectively (Figure S5). For C1s, 281.25 eV indicated the C-O bond and 281.85eV indicated the C=O, which was derived from polyvinyl alcohol and urea[21,28], respectively. 289.7eV indicated the COOH bond from the urea[14], and 290. 4 eV indicated the pie-pie bond of the carbon[16]. (Figure 2A) For N1s, 406.3 eV indicated the N-O bond, the three N-O bonds, corresponding to the urea[20], 405.9 eV for the oxidized N, resulted in the interaction between Fe ion[22](Figure 2B). 396.3eV implied the Fe-N bond [19,26], formed by the urea and the iron ion (Figure 2B). In O1s, 527.1 indicated $O^{2-}$ ion bonded, possibly with the Fe atoms, or generating new iron oxide one as the result of the Fe-O bond[23,27]. 529.25 eV was associated with the lattice oxygen (O1)[15], 534.6 eV was related to the hydroxyl surface, in the case of the hydroxyl group on the polyvinyl alcohol (Figure 2C)[12,22]. In Fe2p, oxidized $Fe^{3+}$ was found on 725.2eV, a result of the interaction with other atoms[11]. $Fe^{2+}$ ion in the $Fe–N_3$ coordination structure was found on 709.4 eV [18], thus Fe-N peaks were located on both N1s and the Fe2p graph (Figure 2D). Through the XPS analysis, it has been concluded that the OC nanozyme contains a partially mimicked, cofactor-like structure. This also implied that the iron was not simply entrapped in the framework but rather provided the certain bond that generates the 'active site'.

**Enzymatic catalytic activity of OC nanozyme**

To designate this organic particle as a nanozyme, the colorimetric assay was conducted to confirm its enzyme-like catalytic activity (Figure 3). Since the core metallic ion selected in this OC nanozyme was iron, thus having peroxidase-activity is the promising output of the OC nanozyme. The colouring substrate ABTS was used for conducting the two-step colorimetric reaction (Figure 3A). The TMB also worked on the

 

OC nanozyme as a substrate, but ABTS has more affinity compared to the TMB as it has less measurement noise but clearly identifies OC nanozyme's peroxidase-like activity (Figure S6). It was confirmed that the iron located in OC nanozyme was the only resource to exhibit catalytic activity due to the Fenton-like reaction; the PVA and urea did not have catalytic activity themselves (Figure 3B).The OC nanozyme was tested to verify its peroxidase-like activity, whether it breaks down the $H_2O_2$ and leads to the ABTS oxidation (Figure 3C). Both absorbance spectra and the absorbance peak have been obtained parallelly, the LOD range was below 100nM (Figure S7). The steady-state kinetic assay was validated utilizing the two substrates: $H_2O_2$ and ABTS. To minimize the measurement noise attributed to ABTS for the kinetic assay, the diluted $H_2O_2$ concentration was selected for the steady-state kinetic assay. The values were calculated through the conventional Michaelis-Menten equation, obtaining the substrate affinity. The $K_m$ of OC nanozyme on $H_2O_2$ was 0.056 mM, and the $K_m$ of OC nanozyme on ABTS was 1.88mM (Figure 3 D, E and SI Table 1). To calculate the $K_{cat}$, the particle concentration obtained from NTA analysis was used. Thus, the calculated $K_{cat}$ of the $H_2O_2$ on OC nanozyme was 1.6 $\times 10^5$. In comparison to the

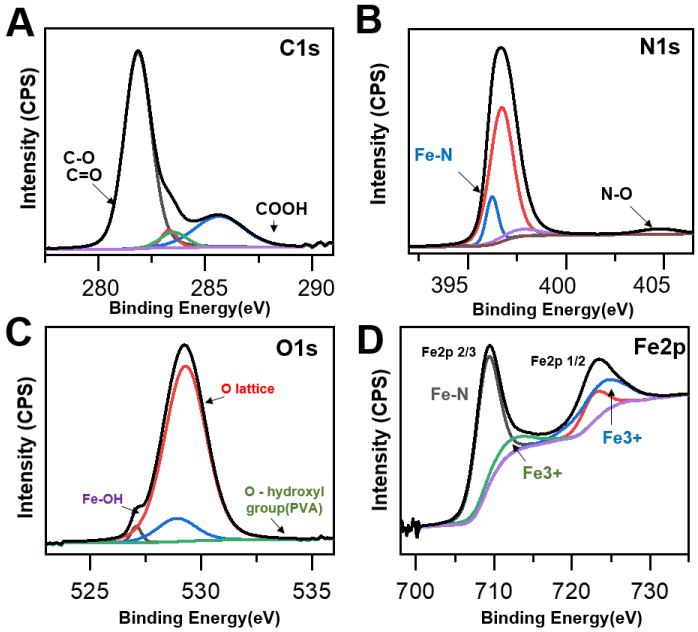


**Fig.2** XPS spectra of OC nanozyme. A) C1s (277eV-293eV), B) N1s (394 eV-407eV), C) O1s (523eV-537eV), D) Fe2p(698eV-735eV).

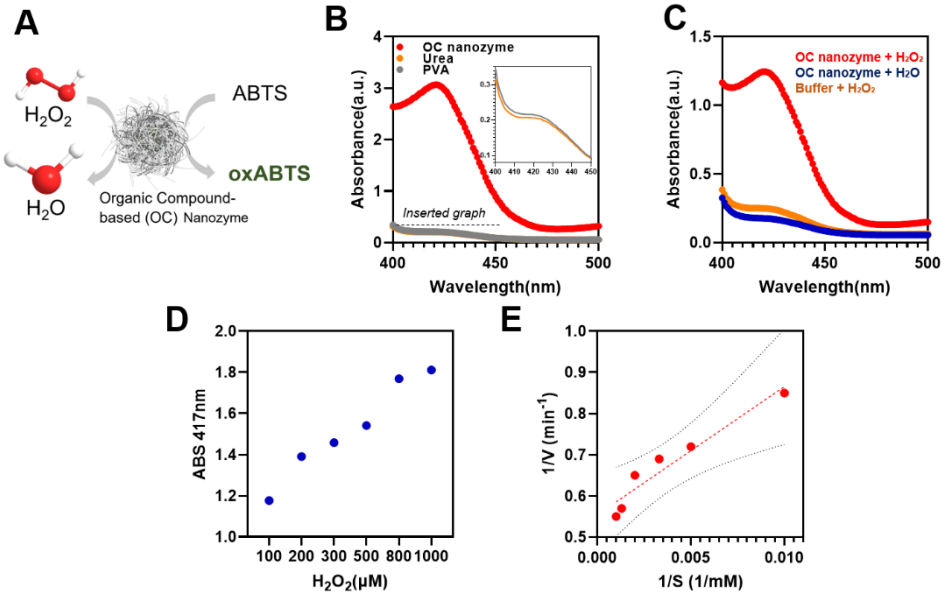


**Fig. 3** Peroxidase-like activity on OC nanozyme. A) schematics of the OC nanozyme- $H_2O_2$-ABTS colorimetric reaction, B) Absorbance spectra of OC nanozyme and the urea and PVA (with $H_2O_2$-ABTS) for the verification of non-catalytic activity of pure urea and the PVA (Inserted graph: Absorbance spectra of urea and PVA from 400-450 nm) , C) Absorbance spectra of OC nanozyme- $H_2O_2$-ABTS of the selective peroxidase-like activity, D and E) Steady state kinetic analysis of OC nanozyme (Substrate: $H_2O_2$)., *N=3.*

references cited in Table S1, the OC nanozyme exhibits decent substrate affinity and an excellent turnover rate. Besides, the pH stability was tested to determine whether it loses its activity due to the incubation under a variety of pH conditions. The pH stability of the OC nanozyme was evaluated by incubating it for a duration of 5 hours in various buffers, and the catalytic activity of the nanozyme remained relatively consistent across a wide pH range. From pH 2 to pH 8.5. This indicates that the OC nanozyme exhibits moredate stability under acid to neutral pH conditions (Figure S8).

**Detection of glyphosate using OC nanozyme integrated with a colorimetric assay**

To prove its potential for agricultural applications, the glyphosate-OC nanozyme-$H_2O_2$-ABTS assay was conducted (Figure 4). As it was confirmed that the OC nanozyme has a peroxidase-like activity with a decent kinetic profile, it was applied to agricultural biomolecule detection with the colorimetric assay platform. For certain herbicides, for instance, it was found that glyphosate has radical scavenging activity indirectly which may interfere with the oxidation of ABTS. In other words, glyphosate compounds reduce the maximum absorbance peak when located on the OC nanozyme/$H_2O_2$/colouring substrate system as they interfere with the direct oxidation of colouring substrate derived from the radical generated by hydrogen peroxide (Figure 4A). Glyphosate detection was conducted with ABTS colorimetric assay with the OC nanozyme−ABTS−$H_2O_2$ system (glyphosate) as follows. The oxidation of the ABTS molecule was measured by varying the concentrations of glyphosate range between 1 ngmL$^{-1}$ to 100 µgmL$^{-1}$ (Figure 4B). A linearity between the concentration of glyphosate and the absorbance peak at 417nm was identified.

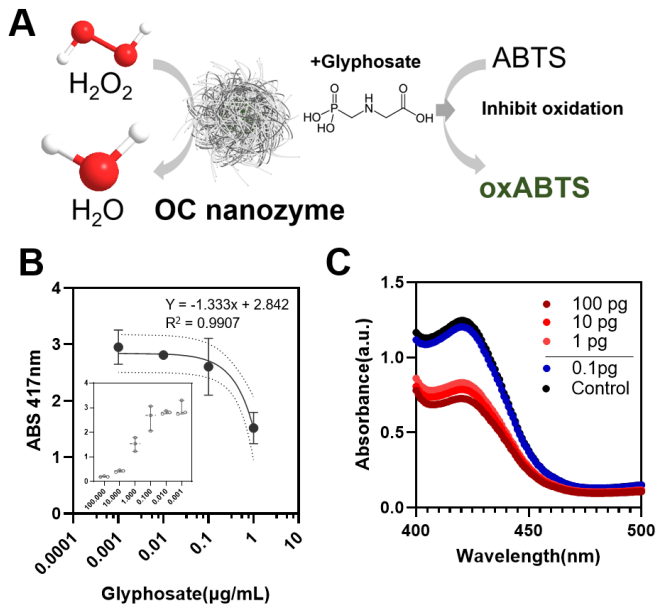


**Fig 4.** Colorimetric glyphosate detection through OC nanozyme- $H_2O_2$-ABTS assay. A) Illustrated strategy of the glyphosate detection, B) Absorbance endpoint measurement of the glyphosate (Inserted graph /1ngmL$^{-1}$-100 µgmL$^{-1}$) and the linearity analysis (1ngmL$^{-1}$-1µgmL$^{-1}$), X axis: log scaled, *N=3*, C) Absorbance spectra for the LOD measurement (black: Control/without glyphosate).

This was applicable with the range of glyphosate concentration in 1ng mL$^{-1}$ to 1 µg mL$^{-1}$ and $R^2$ value was 0.9907. The LOD was obtained from an additional experiment, lowering the $H_2O_2$ concentration 10 times to reduce the fast oxidation of the ABTS.

A differentiable absorbance peak was observed at the 1pg mL$^{-1}$ border, leading us to conclude that the LOD for the system was at least 1pgmL$^{-1}$ (0.001ngmL$^{-1}$) for glyphosate, which implied a decent sensing performance compared to the conventional nanozyme-based sensor for glyphosate detection[9,10,30].

## Conclusions

The self-assembled organic compound-based nanostructures have been synthesized that rely on the chelation of iron with functional groups from urea and polyvinyl alcohol, promoting the one-pot synthesis of the nanozyme. Since there were abundant and heterogenous iron-based ligand elements, it was found that OC the nanozyme exhibits a decent kinetic profile, corresponding to the high density of the 'active site'. Due to OC nanozyme's decent enzyme-like catalytic performance, it successfully detects glyphosate with a decent LOD. Since the OC the nanozyme was prepared from an organic compound which dominantly forms its framework, the authors expect it to be eco-friendly and suitable for direct agricultural application.

## Author Contributions

Dong Hoon Lee: Conceptualization, Formal Analysis, Investigation, Methodology, Writing -Original draft, Writing-Review & Editing.

Mohammed Kamruzzaman: Conceptualization, Supervision, Writing -Original draft, Writing-Review & Editing.

## Abbreviation

| | |
|---|---|
| DLS | Dynamic Light Scattering |
| XPS | X-ray Photoelectron spectroscopy |
| STEM | Scanning transmission electron microscopy |
| SEM | Scanning electron microscopy |
| EDS | Energy-dispersive X-ray spectroscopy |
| ABTS | (2,2'-azino-bis(3-ethylbenzothiazoline-6-sulfonic acid)) |
| TMB | (3,3',5,5'-Tetramethylbenzidine) |
| PVA | Poly (vinyl alcohol) |

## Conflicts of interest

There are no conflicts to declare.

## Acknowledgements

We appreciate the experimental and research support provided by the Material Research Laboratory, High-Throughput Screening facility (utilization of BioTek Cytation 5

Multi-mode Imaging Reader, funded by the office of the Director, National Institutes of Health, award # S10 OD025289), and Beckman Institute at the University of Illinois at Urbana-Champaign. We appreciate the ABE Department and the Department Head for providing the necessary space for the 'Illinois Nanozyme Engineering Lab (INEL)'.

## References

1. C. Peng, R. Pang, J. Li and E. Wang, *Advanced Materials*, 2023, 2211724.
2. H. Wei, L. Gao, K. Fan, J. Liu, J. He, X. Qu, S. Dong, E. Wang and X. Yan, *Nano Today*, 2021, 40.
3. R. Zhang, X. Yan and K. Fan, *Acc Mater Res*, 2021, 2, 534–547.
4. W. Gao, J. He, L. Chen, X. Meng, Y. Ma, L. Cheng, K. Tu, X. Gao, C. Liu, M. Zhang, K. Fan, D. W. Pang and X. Yan, *Nat Commun*, , DOI:10.1038/s41467-023-35828-2.
5. G. Tang, J. He, J. Liu, X. Yan and K. Fan, *Exploration*, 2021, 1, 75–89.
6. Y. Tang, W. Gou, X. Lv, X. Zhou, J. Hao, C. Sun, T. Sun, L. Hu and Z. Yan, *Food Chem*, , DOI:10.1016/j.foodchem.2022.135259.
7. J. Kuang, J. Ju, Y. Lu, Y. Chen, C. Liu, D. Kong, W. Shen, H. W. Shi, L. Li, J. Ye and S. Tang, *Food Chem*, DOI:10.1016/j.foodchem.2023.135856.
8. D. Jiang, D. Ni, Z. T. Rosenkrans, P. Huang, X. Yan and W. Cai, *Chem Soc Rev*, 2019, 48, 3683–3704.
9. X. Luo, G. Huang, C. Bai, C. Wang, Y. Yu, Y. Tan, C. Tang, J. Kong, J. Huang and Z. Li, *J Hazard Mater*, , DOI:10.1016/j.jhazmat.2022.130277.
10. H. Li, S. Zhao, Z. Wang and F. Li, *Small*, , DOI:10.1002/smll.202206465.
11. Z. Wang, H. Jin, T. Meng, K. Liao, W. Meng, J. Yang, D. He, Y. Xiong and S. Mu, *Adv Funct Mater*, , DOI:10.1002/adfm.201802596.
12. W. Liu, J. Zhou, D. Liu, S. Liu and X. Liu, *Mater Lett*, , DOI:10.1016/j.matlet.2021.131076.
13. X. Yin, H. T. Chung, U. Martinez, L. Lin, K. Artyushkova and P. Zelenay, *J Electrochem Soc*, 2019, 166, F3240–F3245.
14. J. Bai, W. Ge, P. Zhou, P. Xu, L. Wang, J. Zhang, X. Jiang, X. Li, Q. Zhou and Y. deng, *J Colloid Interface Sci*, 2022, 616, 433–439.
15. A.Farajollahi, A. Poursattar Marjani, N. Noroozi Pesyan and H. Alamgholiloo, *Appl Surf Sci*, DOI:10.1016/j.apsusc.2023.156903
16. Y. Peng, H. Wang, Q. Li, L. Wang, W. Zhang, L. Zhang, S. Guo, Y. Liu, S. Liu and Q. Ma, *Mater Des*, DOI:10.1016/j.matdes.2022.110522.
17. X. Luo, G. Huang, C. Bai, C. Wang, Y. Yu, Y. Tan, C. Tang, J. Kong, J. Huang and Z. Li, *J Hazard Mater*, DOI:10.1016/j.jhazmat.2022.130277.
18. B. Mecheri, V. C. A. Ficca, M. A. Costa de Oliveira, A. D'Epifanio, E. Placidi, F. Arciprete and S. Licoccia, *Appl Catal B*, 2018, 237, 699–707.
19. Z. Zhang, D. Li, J. Wang and J. Jiang, *Appl Catal B*, DOI:10.1016/j.apcatb.2022.122164.
20. Z. Kamal, M. Zarei Ghobadi, S. M. Mohseni and H. Ghourchian, *Biosens Bioelectron*, DOI:10.1016/j.bios.2021.113334.
21. H. Sepehrmansourie, H. Alamgholiloo, N. Noroozi Pesyan and M. A. Zolfigol, *Appl Catal B*, DOI:10.1016/j.apcatb.2022.122082.
22. Agarwal and B. R. Sankapal, *Chemical Engineering Journal*, DOI:10.1016/j.cej.2021.130131.
23. Y. Wang, S. Zhao, Y. Zhu, R. Qiu, T. Gengenbach, Y. Liu, L. Zu, H. Mao, H. Wang, J. Tang, D. Zhao and C. Selomulya, *iScience*, ,
24. J. Chang, L. Yu, T. Hou, R. Hu and F. Li, *Anal Chem*, 2023, 95, 4479–4485.
25. W. Su, N. Yan, F. Liu, Z. Liu, G. Zhu, S. Wang, X. Liu and W. Wang, *Journal of Physical Chemistry C*, 2022, 126, 4826–4835.
26. S. Zhong, X. Yang, L. Chen, N. Tsumori, N. Taguchi and Q. Xu, *ACS Appl Mater Interfaces*, 2021, 13, 46749–46755.
27. D. Di Girolamo, F. Matteocci, F. U. Kosasih, G. Chistiakova, W. Zuo, G. Divitini, L. Korte, C. Ducati, A. Di Carlo, D. Dini and A. Abate, *Adv Energy Mater*, DOI:10.1002/aenm.20190164
28. K. Guo, F. Shaik, J. Yang, X. Ren and B. Jiang, *J Electrochem Soc*, 2021, 168, 062512.
29. X. W. Song, S. Zhang, H. Zhong, Y. Gao, L. A. Estudillo-Wong, N. Alonso-Vante, X. Shu and Y. Feng, *Inorg Chem Front*, 2021, 8, 109–121.
30. J. Chang, L. Yu, T. Hou, R. Hu and F. Li, *Anal Chem*, 2023, 95, 4479–4485.